Hemicalcin, a new toxin from the Iranian scorpion *Hemiscorpius lepturus* which is active on ryanodine-sensitive Ca^{2+} channels

Delavar SHAHBAZZADEH*†[1], Najet SRAIRI-ABID*[1,2], Wei FENG‡, Narendra RAM§, Lamia BORCHANI*, Michel RONJAT§, Abolfazl AKBARI‖, Isaac N. PESSAH‡, Michel DE WAARD§ and Mohamed EL AYEB*

*Laboratoire des Venins et Toxines, Institut Pasteur de Tunis, 13 place Pasteur, Tunis, BP-74, 1002 Tunisia, †Biotechnology Department, Institute Pasteur of Iran, P.O. Box 13164, Tehran, Iran, ‡Department of Veterinary Medicine-Molecular Biosciences and Center for Children's Environmental Health, University of California Davis, One Shields Avenue, Davis, CA 95616, U.S.A., §INSERM U607, Canaux Calciques, Fonctions et Pathologies, Département Réponse et Dynamique Cellulaire, Commissariat à l'Energie Atomique, 17 rue des Martyrs, 38054 Grenoble Cedex 09, France, and ‖Razi Vaccine & Serum Research Institute, 31975/148 Karaj, Iran

In the present work, we purified and characterized a novel toxin named hemicalcin from the venom of the Iranian chactoid scorpion *Hemiscorpius lepturus* where it represents 0.6 % of the total protein content. It is a 33-mer basic peptide reticulated by three disulfide bridges, and that shares between 85 and 91 % sequence identity with four other toxins, all known or supposed to be active on ryanodine-sensitive calcium channels. Hemicalcin differs from these other toxins by seven amino acids at positions 9 (leucine/arginine), 12 (alanine/glutamic acid), 13 (aspartic acid/asparagine), 14 (lysine/asparagine), 18 (serine/glycine), 26 (threonine/alanine) and 28 (proline/isoleucine/alanine). In spite of these differences, hemicalcin remains active on ryanodine-sensitive Ca^{2+} channels, since it increases [^{3}H]ryanodine binding on RyR1 (ryanodine receptor type 1) and triggers Ca^{2+} release from sarcoplasmic vesicles. Bilayer lipid membrane experiments, in which the RyR1 channel is reconstituted and its gating properties are analysed, indicate that hemicalcin promotes an increase in the opening probability at intermediate concentration and induces a long-lasting subconductance level of 38 % of the original amplitude at higher concentrations. Mice intracerebroventricular inoculation of 300 ng of hemicalcin induces neurotoxic symptoms *in vivo*, followed by death. Overall, these data identify a new biologically active toxin that belongs to a family of peptides active on the ryanodine-sensitive channel.

Key words: dihydropyridine receptor (DHPR), hemicalcin (HCa), *Hemiscorpius lepturus*, homology modelling, ryanodine receptor (RyR), scorpion toxin.

INTRODUCTION

Hemiscorpius lepturus is the most dangerous scorpion of Khuzestan, the south-west, hot and humid province of Iran. Of all scorpion stings, 10–15 % during the hot season and almost all cases during the winter are due to *H. lepturus*. These observations are based on a sample of 2534 patients who brought a scorpion specimen to a medical centre while seeking treatment [1]. In addition to inducing typical symptoms of necrosis and ulceration of the skin and haemolysis of blood cells, *H. lepturus* venom exerts its most toxic effects on the CNS (central nervous system) and cardiovascular system [1]. Scorpion peptides that possess neurotoxic activity in mice are generally known to modulate Na^+, K^+ or Ca^{2+} channels. Calcium channels have been classified into various subfamilies, including voltage-gated channels, voltage-independent channels and intracellular endoplasmic/SR (sarcoplasmic reticulum) calcium release channels. The latter channels include the ryanodine receptors (RyRs), whose openings can be induced by Ca^{2+} itself or by an allosteric coupling with the plasmalemmal DHPR (dihydropyridine receptor) [2,3]. Only a few scorpion venom peptides have been identified as possessing activity towards RyRs. *Pandinus imperator* venom contains IpTx (imperatoxin) I and A [4,5], whereas *Scorpio maurus* contains MCa (maurocalcine) [6], *Buthus martensii* Karsch contains BmK-PL toxin [7], and *Buthotus judaicus* contains BjTx-1 and BjTx-2 [8]. Although these toxins are potent modulators of RyRs, they are structurally divergent. BjTx-1 and BjTx-2 adopt a classical α/β scaffold, as do many toxins active on voltage-gated K^+ and Na^+ channels [9,10], whereas MCa and IpTx A are the only scorpion toxins that adopt an ICK (inhibitor cystine knot) fold [11,12]. In the present work, we isolated, identified and characterized a new neurotoxic peptide from the Iranian scorpion *H. lepturus*. This toxin, named HCa (hemicalcin), differs from MCa and IpTx A by three and four amino acids respectively. HCa stimulates [^{3}H]ryanodine binding to RyR1, produces Ca^{2+} release from SR vesicles, and triggers significant changes in the biophysical behaviour of RyR1 channels reconstituted in BLMs (bilayer lipid membranes). Compared with MCa, HCa is significantly more toxic to mice *in vivo*. The data presented herein indicate that HCa represents a new member of the small family of toxins active on RyR1.

EXPERIMENTAL

Scorpion venom

Venoms of *H. lepturus* scorpions from Khuzestan (Iran) were collected by the veterinarian service of the Razi Vaccine Development and Serum Research Institute of Iran and kept frozen at −20 °C in their crude forms until use.

Abbreviations used: τ_o, mean open-dwell time; τ_c, mean closed-dwell time; BLM, bilayer lipid membrane; CNS, central nervous system; DHPR, dihydropyridine receptor; F_o, occurrence of subconductance gating; HCa, hemicalcin; ICK, inhibitor cystine knot; i.c.v., intracerebroventricular; IpTx, imperatoxin; MALDI, matrix-assisted laser-desorption ionization; MCa, maurocalcine; P_o, open probability; RyR, ryanodine receptor; SR, sarcoplasmic reticulum; TFA, trifluoroacetic acid.

[1] These authors contributed equally to this work.

[2] To whom correspondence should be addressed (email najet.abid@pasteur.rns.tn).

Purification of HCa

Crude venoms were dissolved in water and loaded on Sephadex G-50 gel-filtration chromatography columns (2 × K26/50) to isolate a neurotoxic fraction. The columns were equilibrated with 20 mM ammonium acetate at pH 4.7. The neurotoxic fraction was identified by i.c.v. (intracerebroventricular) injection in mice. After freeze-drying, the neurotoxic fraction was fractionated using a C_8 reverse-phase HPLC column (5 μm particle size, 4.6 mm × 250 mm) (Beckman Fullerton), equipped with a Beckman Series 125 pump and a Beckman diode array detector set at 214 and 280 nm. Elution was controlled by means of the software Gold®. Proteins were eluted from the column at a flow rate of 0.8 ml/min using a linear gradient (45 min) from 12 to 40 % of solution B [0.1 % TFA (trifluoroacetic acid) in acetonitrile] in solution A (0.1 % TFA in water). The protein concentration was measured by the Bradford method.

In vivo toxicity tests and LD_{50} determination

The *in vivo* toxicity of HCa was tested on 20 ± 2 g C57/BL6 male mice by i.c.v. injection of 5 μl of 0.1 % (w/v) BSA solutions containing increasing amounts of the polypeptides. Six mice were used for each dose; two control mice were injected with only 0.1 % BSA in water, to be sure that symptoms are not due to experimental conditions. Mice were anaesthetized for i.c.v. administration, according to the method described by Galeotti et al. [13]. Experiments on mice were carried out in accordance with the European Community Council Directive (86/609/EEC) for experimental animal care, and all procedures met with the approval of the Institutional Research Board of the Pasteur Institute of Tunis.

Amino acid sequence determination of HCa

Reduction of HCa with dithiothreitol, and alkylation with 4-vinylpyridine, were performed as previously described [14]. The sequence of reduced/carboxymethylated toxin was determined using an automatic liquid-phase protein sequencer (model 476A, Applied Biosystems) using a standard Edman protein degradation. HCa was deposited on to Biobrene-precycled glass-fibre discs.

Mass spectrometry

Samples were analysed on Voyager-DE™ PRO MALDI–TOF (matrix-assisted laser-desorption ionization–time-of-flight) Workstation mass spectrometer (Perseptive Biosystems). The peptide was dissolved in 30 % acetonitrile with 0.3 % TFA to obtain a concentration of 1–10 pmol/μl. The matrix was prepared as follows: α-cyanohydroxycinnamic acid was dissolved in 50 % acetonitrile in 0.3 % TFA to obtain a saturated solution of 10 μg/μl. A 0.5 μl volume of peptide solution was mixed with 0.5 μl of matrix solution and placed on the sample plate, and the mixture was allowed to dry. Mass spectra were recorded in reflectron mode after external calibration with suitable standards and were analysed using the GRAMS/386 software.

Sequence comparison

Peptides showing sequence similarity with HCa were identified with BLAST2 [15] in the non-redundant database. Best hits were calcium channel toxin modulators. The amino acid sequences of these peptides were aligned and identities were determined.

SR vesicle preparation

Heavy SR vesicles were prepared following a method modified from that of Kim et al. [16] as described by Marty et al. [17]. Junctional SR was prepared as described by Pessah et al. [18]. Protein concentration was measured following the method of Lowry or using the Biuret away.

[^{3}H]Ryanodine binding assay

Heavy SR vesicles (1 mg/ml) were incubated at 37 °C for 3 h in an assay buffer composed of 5 nM [^{3}H]ryanodine, 150 mM NaCl, 2 mM EGTA, 2 mM $CaCl_2$ (pCa = 5) and 20 mM Hepes, pH 7.4. HCa was added to the assay buffer just before the addition of heavy SR vesicles. [^{3}H]Ryanodine bound to heavy SR vesicles was measured by filtration through Whatman GF/B glass filters followed by three washes with 5 ml of ice-cold washing buffer composed of 150 mM NaCl and 20 mM Hepes, pH 7.4. Filters were then soaked overnight in 10 ml of scintillation cocktail (Cybscint, ICN), and bound radioactivity was determined by scintillation spectrometry. Non-specific binding was measured in the presence of 20 μM unlabelled ryanodine. Each experiment was performed in triplicate and repeated at least twice. All data are presented as means ± S.D.

Ca^{2+} release measurements

Ca^{2+} release from heavy SR vesicles was measured using antipyrylazo III, a Ca^{2+}-sensitive dye. The absorbance was monitored at 710 nm by a diode array spectrophotometer (MOS-200 Optical System, Biologic). Heavy SR vesicles (25 μg) were actively loaded with Ca^{2+} at 37 °C in 2 ml of buffer containing 100 mM KCl, 7.5 mM sodium pyrophosphate and 20 mM Mops, pH 7.0, supplemented with 250 μM antipyrylazo III and 1 mM ATP/$MgCl_2$. Ca^{2+} loading was started by four sequential additions of 20 μM $CaCl_2$. Under these loading conditions, there was no calcium-induced calcium release to interfere with the effect of HCa on Ca^{2+} release from heavy SR vesicles. At the end of the experiment, the Ca^{2+} released by HCa was chelated by the addition of 1 mM EGTA.

Recording and analysis of RyR1 single-channel activity in BLMs

The BLM was formed across a 200 μm aperture drilled into a polysulfone cup (Warner Instrument Corp.) using a mixture composed of phosphatidylethanolamine/phosphatidylserine/phosphatidylcholine (5:3:2, by wt) (Avanti Polar Lipids) dissolved in decane at a final concentration of 30 mg/ml. The BLM partitioned two chambers (*cis* and *trans*) with buffer solution containing 500 mM CsCl, 7 μM free Ca^{2+} and 20 mM Hepes/Tris (pH 7.4) for *cis*, and 50 CsCl and 20 Hepes/Tris (pH 7.4) for *trans*. The *cis* chamber was virtually grounded, whereas the *trans* chamber was connected to the head stage input of an amplifier (Bilayer Clamp BC 525C, Warner Instrument Corp.). Single channels were obtained by introducing rabbit skeletal muscle junctional SR vesicles or purified RyR1 preparation in the *cis* chamber to induce fusion with the BLM. Immediately after incorporation of a channel into the BLM, the *cis* chamber was perfused with an identical solution to prevent additional vesicle fusions. Single-channel gating was monitored and recorded at a holding potential of −40 mV (applied to the *trans* side). The amplified current signals, filtered at 1 kHz (8 pole low-pass bessel filter, Warner Instrument Corp.), were digitized and acquired at a sampling rate of 10 kHz (Digidata 1320A, Axon-Molecular Devices). All the recordings were made for at least 3 min under each defined condition. The channel open probability (P_o), mean open-, mean closed-dwell times (τ_o and τ_c) and current amplitude histograms were calculated and displayed graphically using Clampfit, pClamp software 9.0 (Axon-Molecular Devices).

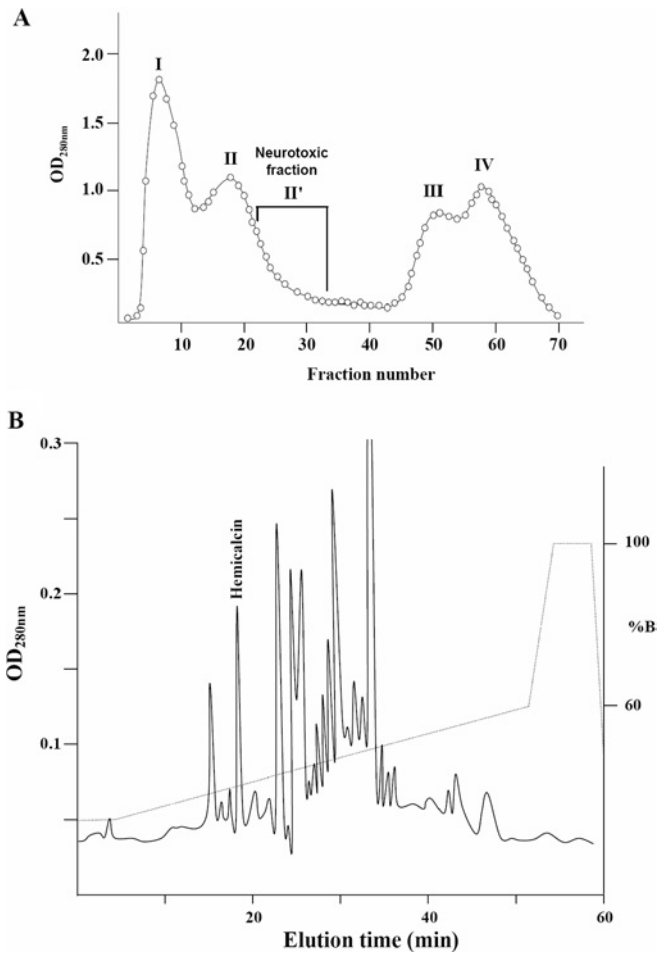

Figure 1 Purification of HCa from the venom of *H. lepturus*

(**A**) The extracted venom was fractionated by G-50 gel-filtration chromatography columns (2 × K26/50) equilibrated with 20 mM ammonium acetate, pH 4.7. (**B**) HCa was purified from the neurotoxic fraction (II') by reverse-phase HPLC on a C_8 column using a gradient of buffer B (0.1 % TFA in acetonitrile) as described in the Experimental section. HCa was collected at 18.93 min. OD_{280nm}, A_{280}.

Molecular modelling

A structural model of HCa was generated by homology modelling with the program Modeller 8v2 [19]. Homologous polypeptides with known structures were identified by a BLAST2 [15] search of the PDB database using the sequence of HCa as the entry. The solution structures of MCa (PDB code 1C6W) [11] and IpTx A (PDB code 1IE6) [12] were used as templates. A total of 20 structures were calculated, from which only one model, combining the best Ramachandran plot (http://swift.cmbi.kun.nl/WIWWWI/ramaplot.html; [20]), and good scores for the objective function values [19], and the VICTOR/FRST energy function proposed by Tosatto [21] (http://protein.cribi.unipd.it/frst/), was selected. The model was then visualized with the ViewerLite50 program (http://www.accelrys.com/products/dstudio/).

RESULTS

Purification of HCa

After Sephadex G50 chromatography of the *H. lepturus* venom, each fraction obtained was injected into the mice by the i.c.v. route, and the neurotoxic fractions were pooled (Figure 1A) and applied to a C_8 HPLC column. HCa was eluted at 18.93 min (Figure 1B). An analytical HPLC run of HCa showed a single symmetrical peak. HCa represents approx. 0.6 % of the *H. lepturus* venom.

In vivo toxicity of HCa

HCa (500 ng in 5 μl) was injected into mice by the i.c.v. route and the following symptoms were observed. The toxin produced rapid paralysis in the lower half of the body. The mice were no longer able to move their heads forward. The mice turned backwards while moving circularly, and their heads were down to the ground and bent to the body. At 5–10 min after injection, the first symptoms disappeared and the mice started to jump and run very fast. This phenomenon took 1–2 min. The animals then stopped moving and started trembling for a while. Next, they took a rest without any movement. Jumping, running and trembling happened every 5–10 min. The last stage was repeated four or five times, and in the last trembling episode, spasms occurred in all muscles and the animals died while their bodies were laid down and their four legs were in a straight position. With sublethal doses of HCa, the same symptoms were observed, except for the very last stage that precedes death. The 50 % killing dose for mice was 300 ng, giving an LD_{50} of 15 μg of toxin/1 kg of mouse.

Sequence determination and comparison with other scorpion toxins

Edman degradation of 2 nmol of S-pyridylethylated peptides led to the identification of the complete amino acid sequence of the peptide (Figure 2). HCa is a peptide composed of 33 amino acid residues containing six cysteine residues. The experimental molecular mass of native HCa (3788.09 $\pm$ 0.67 Da) obtained by MALDI is nearly identical with the average theoretical molecular mass calculated for the fully oxidized form of HCa (3787 Da). These results indicate that the six cysteine residues of HCa are engaged in three intramolecular disulfide bridges. Moreover, only a monomeric form was observed in the mass spectra, suggesting the absence of intermolecular disulfide bridges.

HCa has very strong sequence homologies with MCa from the chactoid scorpion *Scorpio maurus* [6] (91 % sequence identity), with IpTx A from the scorpion *Pandinus imperator* [5] (88 % sequence identity), and with both opicalcine 1 and 2 from the scorpion *Opistophthalmus carinatus* [22] (88 % and 85 % sequence identity respectively) (Figure 2). Among these toxins, variation in amino acid sequence takes place at seven positions (9, 12–14, 18, 26 and 28) without altering the net global charge of the peptides (+8). The alignment of the cysteine residues of HCa with that of MCa and IpTx A indicates that HCa could also possess the typical pairing of disulfide bridges observed in the family of toxins belonging to the family Scorpionidae (Cys^3–Cys^{17}, Cys^{10}–Cys^{21} and Cys^{16}–Cys^{32}).

Like the four other scorpion toxins, HCa also presents sequence homology (21 % identity) with peptide A which is derived from the cytoplasmic II–III loop of the $Ca_v1.1$ subunit of the DHPR (Figure 2B).

[^{3}H]Ryanodine-binding assay

MCa and IpTx A are both known to stimulate the binding of [^{3}H]ryanodine, a biochemical indicator of channel activity, to heavy SR vesicles enriched in RyR1 [5,11]. Considering the sequence homology among these toxins, it is expected that HCa should also enhance [^{3}H]ryanodine binding to RyR1. Figure 3 shows that HCa does indeed increase the binding of [^{3}H]ryanodine in a dose-dependent manner, with an EC_{50} of 71 $\pm$ 6 nM. Under these assay conditions, the binding of [^{3}H]ryanodine on RyR1

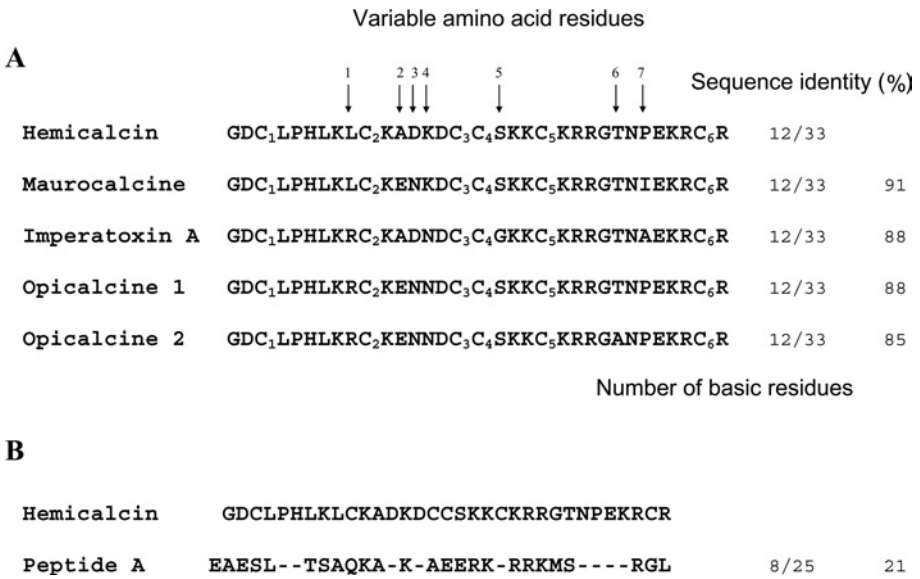

Figure 2 Sequence alignment of HCa with related toxins active on the RyR

(**A**) Sequence alignment of HCa with four analogous toxins, MCa, IpTx A, opicalcine 1 and opicalcine 2. MCa and IpTx A are two peptides known to be active on the RyR. Opicalcine 1 and 2 have not been tested for pharmacological activity. All five toxins have the same number of positively charged amino acid residues (the N-terminal glycine residue, six or seven lysine residues and four or five arginine residues). (**B**) A sequence alignment of HCa with peptide A of the II–III loop of $Ca_v\alpha_{1.1}$ subunit from the DHPR is also provided. The strongest homology stretches from Lys[19] to Thr[26] of HCa.

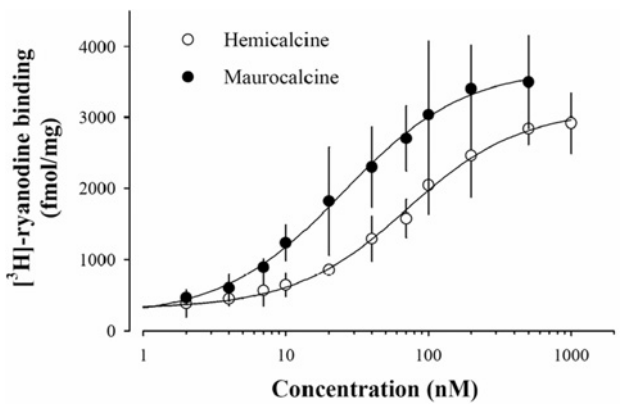

Figure 3 HCa affects [^{3}H]ryanodine binding on heavy SR vesicles

Dose-dependent effect of HCa on [^{3}H]ryanodine binding on to heavy SR vesicles (○). [^{3}H]Ryanodine binding was measured at pCa 5 in the presence of 5 nM [^{3}H]ryanodine for 3 h at 37 °C. Non-specific binding remained constant at all HCa concentrations and was less than 200 fmol/mg. Data were fitted with a logistic function $y = y_0 + \{a/[1 + (x/EC_{50})^b]\}$ where $y_0 = 316 \pm 46$ in the absence of HCa, $a = 2799 \pm 118$ fmol/mg is the maximum [^{3}H]ryanodine binding, $b = -1.1 \pm 0.1$ (the slope coefficient), and $EC_{50} = 71 \pm 6$ nM (the concentration of HCa for half stimulation of [^{3}H]ryanodine binding). Overall, HCa stimulates [^{3}H]ryanodine binding 11.8-fold at saturation level. For comparison, the data are also shown for MCa (●; $y_0 = 364 \pm 129$, $a = 3502 \pm 127$ fmol/mg, $b = -1.0 \pm 0.1$, and $EC_{50} = 25 \pm 2$ nM; stimulation factor of 16.7 at saturation).

was stimulated 11.8-fold at saturating concentrations of HCa. In comparison, MCa was slightly more effective than HCa, since it increased [^{3}H]ryanodine binding 16.7-fold, with an EC_{50} of 25 ± 2 nM.

Enhancement of Ca^{2+} release from SR

In order to investigate the effect of HCa on Ca^{2+} release from heavy SR vesicles, we first determined that the purified HCa did not contain any significant Ca^{2+} concentration that could affect the interpretation of Ca^{2+} release measurements induced by the peptide. Absorbance measurements indeed illustrated the absence of significant Ca^{2+} concentrations upon addition of 40 nM HCa (Figure 4A). Next, we actively loaded the SR vesicles by four consecutive additions of Ca^{2+} (20 μM) in the presence of ATP-Mg^{2+}, pyrophosphate and ATP-regenerating system. After Ca^{2+} loading reaches equilibrium, addition of 125 nM HCa along with 20 μM Ca^{2+} to the external medium induces Ca^{2+} release, as shown in Figure 4(B). The HCa response comes with slower up-rise kinetics than the added Ca^{2+}, again indicating that it could not be linked to contaminating Ca^{2+} from the purified material. External Ca^{2+} level reached a plateau, indicating that near-maximal Ca^{2+} release had occurred. Ca^{2+} was added along HCa, as it appears to promote the effect of the peptide. The remaining Ca^{2+} from the SR vesicles could be released by the application of 1 μM A23187 ionophore. Further application of 20 μM external Ca^{2+} was not taken up by the vesicles, consistent with the effect of the ionophore in SR vesicles, which is to produce continuous Ca^{2+} leakage from the vesicles. The external Ca^{2+} concentration could be lowered by the application of 0.5 mM external EGTA. The Ca^{2+} specifically released by HCa from the SR vesicles amounted to 47.7 ± 15.1 nmol ($n = 3$) and represented 66 ± 18 % of the total calcium stored by the vesicles. As control experiments, and in order to make sure that the fifth application of 20 μM Ca^{2+} is not responsible for the large response of HCa, an experiment was performed in which five consecutive additions of 20 μM Ca^{2+} were applied to SR vesicles (Figure 4C). As indicated, 20 μM Ca^{2+} alone for the fifth application did not produce a response similar to 20 μM Ca^{2+} along with HCa. This was also not the case when the fifth application was 40 μM Ca^{2+}, totally disproving the idea that HCa is contaminated with calcium. Overall, these results are similar to those previously observed with MCa and IpTx A, indicating a possible direct effect of HCa on RyR1 [23,24]. To illustrate this point further, the effect of HCa on RyR1 channel activity was investigated.

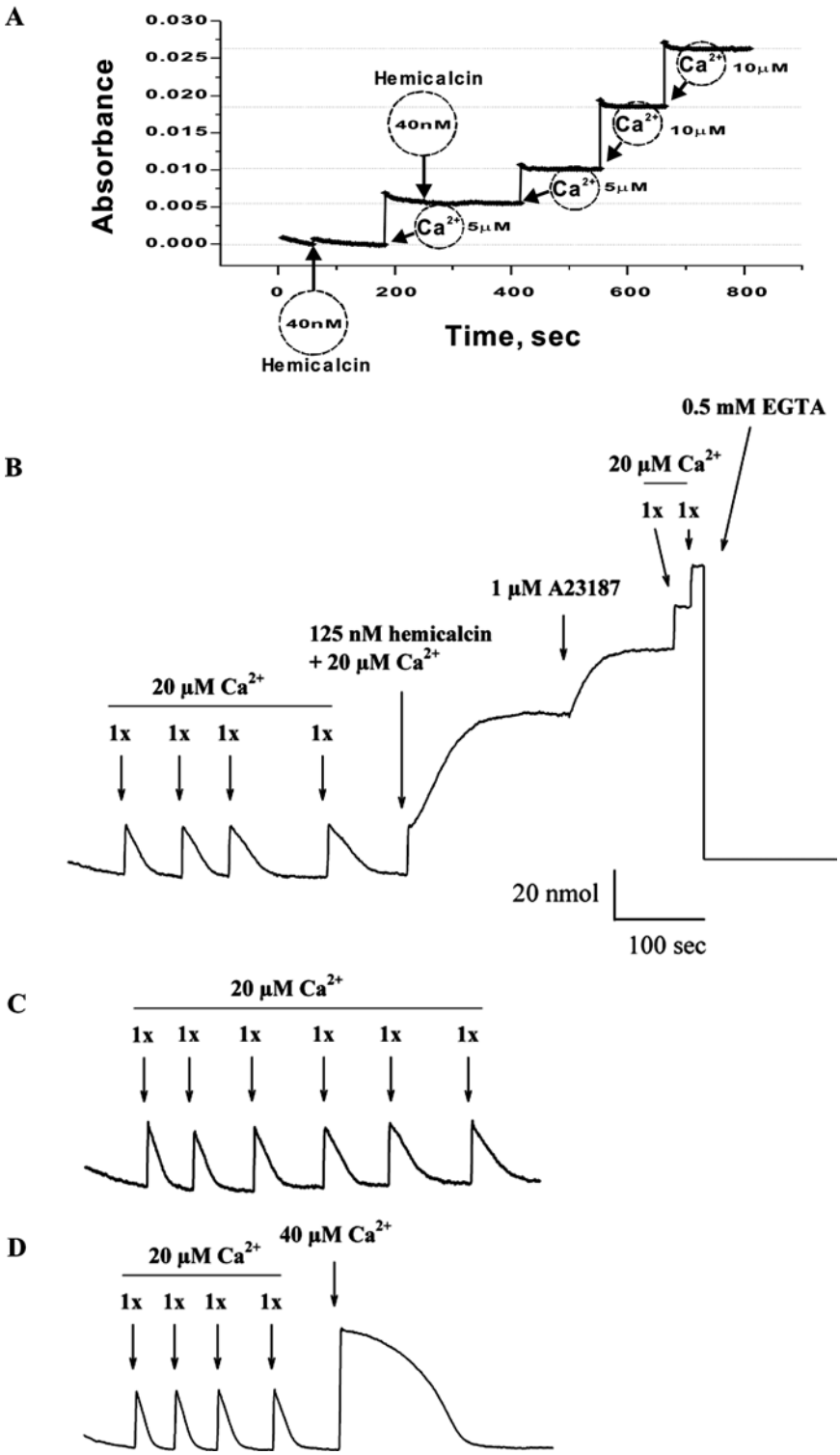

Figure 4 Ca^{2+} release from heavy SR vesicles induced by HCa

(**A**) Absorbance measured in the absence of SR vesicles and in response to sequential Ca^{2+} additions in the medium or to 40 nM HCa addition. The data indicate the lack of Ca^{2+} in the purified material. (**B**) Heavy SR vesicles were actively loaded with Ca^{2+} by four sequential additions of 20 μM $CaCl_2$ in the monitoring chamber. The absorbance was monitored to show that the added Ca^{2+} was taken up by the SR vesicles. The trace relaxed close to its original baseline with $CaCl_2$ additions constituting approx. 70–80 % of the SR loading capacity. These Ca^{2+} additions were used to calibrate the Ca^{2+} release. Addition of 125 nM HCa produces a long-lasting Ca^{2+} release from SR vesicles. Ca^{2+} (20 μM) was added along with HCa to control the extravesicular concentration of Ca^{2+}. Also, external Ca^{2+} appears to act as a cofactor to the HCa effect. Residual Ca^{2+} from SR vesicles is released by the addition of 1 μM ionophore A23187. Further addition of 0.5 mM EGTA buffers the released and the basal Ca^{2+} from the system. (**C**) Loading of heavy SR vesicles with Ca^{2+} by six sequential additions of 20 μM $CaCl_2$ in the monitoring absorbance chamber. The fifth application did not produce a similar calcium release to the one observed by the co-application of 20 μM Ca^{2+} and 125 nM HCa in (**B**). (**D**) Loading of heavy SR vesicles with Ca^{2+} by four sequential additions of 20 μM $CaCl_2$ and a fifth one at 40 μM in the monitoring absorbance chamber. The fifth application produces a slower loading of the vesicles, but no sustained response.

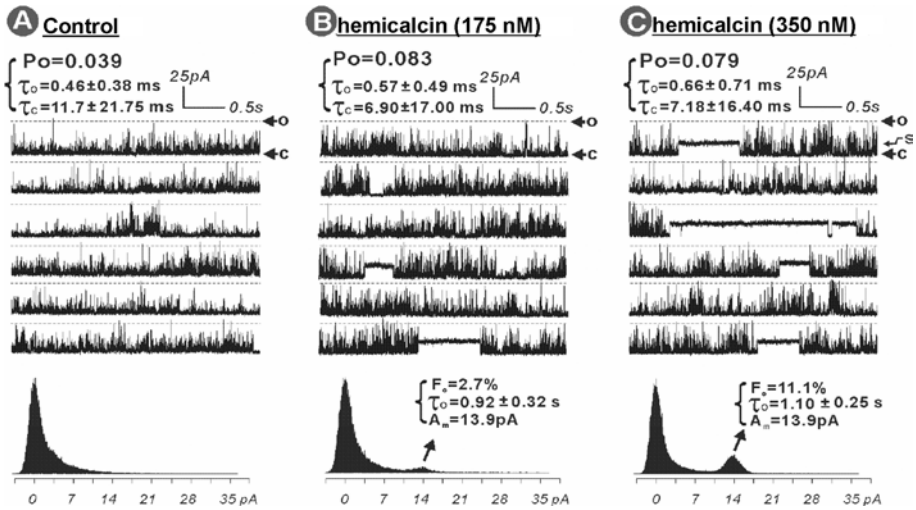

Figure 5 HCa alters gating kinetics and stabilizes subconductances of RyR1 single-channel activity in BLMs

RyR1 single channel was incorporated by inducing fusion of skeletal muscle junctional SR vesicles into BLMs. The channel activities were recorded and analysed as described in the Experimental section. RyR1 single channel in the absence of HCa was used to serve as control and was recorded for 3 min (**A**). Sequential additions of HCa to achieve a final concentration of 175 nM (**B**) and 350 nM (**C**) were made into the *cis* chamber, and the channel activity was recorded for 5 min under each condition. The broken lines indicate the maximum current amplitude of the native RyR1 channel (37.2 pA) when the channel is fully open (o). The arrow marked 'c' shows the zero current level when the channel is in the fully closed state, and the arrow marked 's' shows the HCa-stabilized subconductance state of the channel. The data are representative of a total of five independent bilayer experiments with RyR1 channels from one junctional SR protein preparation and one purified RyR1 preparation.

Effects of HCa on RyR1 channel activity

The mechanism by which HCa influences RyR1 channel activity was assessed further by measuring the effects of the toxin on the gating parameters of single channels reconstituted into BLMs. Figure 5 shows a RyR1 channel in the presence of 7 μM cytosolic Ca^{2+} before (Figure 5A) and after (Figures 5B and 5C) being exposed to nanomolar concentrations of HCa. In the absence of HCa, the channel exhibited low activity, with a P_o of 0.039 (Figure 5A). However, addition of 175 nM HCa into *cis* solution rapidly activated the channel, promoting a 2.1-fold increase of the P_o to 0.083 and moderate changes in both the mean τ_o and τ_c values: τ_o increased by 124 %, whereas τ_c decreased by 59 %. A prominent effect of HCa (175 nM) on channel gating behaviour was stabilization of an occasional long-lasting subconductance state. Amplitude histogram analysis indicates that the predominant HCa-modified subconductance state was ~38 % of the full state of 37.2 pA. The HCa-modified channel displayed a τ_o of 0.92 ± 0.32 s, more than 1600-fold longer than that of the native RyR1 channel gating mode. The occurrence of this subconductance gating (F_o) is ~2.7 % (the percentage of the time that the channel gates in a subconductance state compared with total time, all-mode gating states). A higher concentration of HCa (350 nM final concentration in *cis* solution, Figure 5C) did not further significantly change the P_o, τ_o or τ_c, but resulted in more frequent appearance of the long-lasting subconductance gating mode: F_o increased more than 4-fold, from 2.7 to 11.1 %. The subsequent addition of ryanodine (125 μM) into the *cis* solution of the HCa-modified channel, rapidly stabilized a substate approx. 60 % of the full conductance state (ryanodine-modified substate), with frequent closures to a current level 20.9 % of the maximum current level (ryanodine + HCa-modified state). Under these conditions, the channel shut down completely within 45 s (results not shown).

In other BLM experiments, 50 nM HCa was found to produce negligible effects on RyR1 channel gating kinetics ($n = 3$), whereas, at 100 nM, the toxin slightly increased P_o and induced the occasional appearance of long-lasting subconductance gating mode, indicating that the effects of HCa on channel gating are dose-dependent (results not shown).

Molecular model of HCa

The molecular model of HCa was established by homology modelling using solution structures of MCa and IpTx A as templates. The molecular model of HCa is shown along with the three-dimensional solution structure of MCa (Figure 6A). As expected, the fold of the HCa model appears to be very similar to the folding of the template experimental structure, i.e. a compact disulfide-bonded core from which several loops and the N-terminus emerge. The main elements of regular secondary structure are a double-stranded antiparallel β-sheet comprising residues 20–22 and 30–33, a third peripheral extended strand composed of residues 8–10, which is almost perpendicular to the double-stranded antiparallel β-sheet, and a helical turn composed of residues 13–15. Thus the model suggests that HCa probably folds according to the ICK described previously in MCa [11] and IpTx A [12].

DISCUSSION

In the present study, we isolated the first toxin from the venom of the Iranian scorpion *Hemiscorpus lepturus*, herein termed hemicalcin (HCa). It is a highly basic 33-amino-acid peptide that is cross-linked by three disulfide bridges. It shares approx. 90 % sequence identity with MCa and 88 % with IpTx A. Like these two related toxins, HCa also shares sequence homology with peptide A, a domain of the II–III loop of $Ca_v1.1$, a dihydropyridine-sensitive voltage-dependent calcium channel of the skeletal muscle. A common binding site on RyR1 that can bind peptide A as well as MCa indicates that the binding of these toxins on RyR1 involves the region of homology between peptide A and the toxins [25]. Peptide A induces Ca^{2+} release from the SR and enhances current flow through RyR1 channels [5,26–28]. The ability of peptide A to activate RyR1 is highly related to the orientation of its positively charged residues along one face of the molecule [28]. Both IpTx A and MCa also share a similar orientation of positively charged residues with peptide A in this surface [11,28], indicating that the same basic domain at the surface of these peptides is most likely to be involved in the activation of the

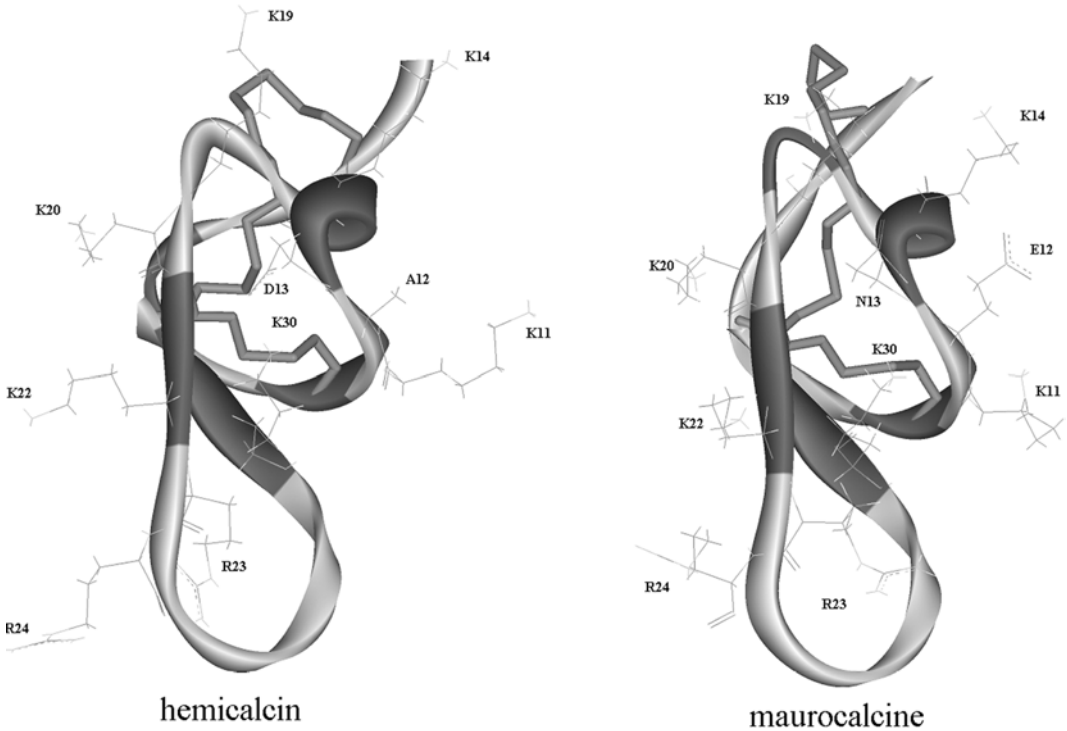

Figure 6 Homology model of HCa

Backbone ribbon representation of the model of HCa and comparison with the structure of MCa (PDB code 1C6W [11]), which, besides IpTx A, is one of the two structures used as template for molecular modelling. Disulfide bridges are in stick representation. Basic amino acid residues present on the same face of MCa and HCa (Lys^{19}, Lys^{20}, Lys^{22}, Arg^{23} , Arg^{24} and Lys^{30}) are shown. The side-chain bonds of Lys^{11}, Lys^{14}, Asp^{13} and Ala^{12} in HCa and Lys^{11}, Lys^{14}, Asn^{13} and Glu^{12} in MCa are also shown.

RyR1 channel. The molecular model of HCa suggests that it also possesses a highly basic domain that presents the same surface orientation as in IpTx A and MCa. Because of its high homology with peptides that are active on RyR1 channels, we expected that HCa could be able to activate this channel type too. Indeed, HCa was found to increase [^{3}H]ryanodine binding on RyR1 with an apparent EC_{50} of 71 ± 6 nM. In comparison, HCa was found to be almost as potent as MCa for stimulating [^{3}H]ryanodine binding. Also, application of 50 nM HCa on SR loaded with Ca^{2+} produced a significant Ca^{2+} release. Enhanced release of Ca^{2+} and specific [^{3}H]ryanodine binding are due to a direct effect of HCa on the gating properties of the RyR1 channel, since the peptide induces an increase in P_o and, at higher concentrations, stabilizes a long-lived subconductance state. These results show that the activity of HCa on RyR1 Ca^{2+} channels is similar to those observed with the two other toxins characterized hitherto, indicating that these toxins have similar mechanisms of action on RyR1. However, the predominant subconductance level that HCa induces (38 % of full conductance) differs significantly from those measured with MCa ($\sim$48–54 % of full conductance [23,24]) or IpTx A (25 % of full conductance [29,30]). The functional differences observed among these toxins must be endowed by their structural differences.

Structure–function relationships of calcium channel scorpion toxins, especially on RyR isoform specificity, are not yet well defined, because only few members of these toxins were found within a scorpion species. Until now, only two toxins, MCa and IpTxA (from *Scorpio maurus* and *Pandinus imperator* scorpions respectively), derived from orthologous genes, have been studied. The discovery of new natural toxins from related species might give access to active structures displaying multipoint mutations compared with these two toxins and may bring useful information in structure–function relationships. Previous studies on synthetic monosubstituted analogues of MCa showed that some amino acid residues of MCa can be classified into three different groups: (i) residues belonging to the basic class that are important for interaction with RyR1 (Lys^{22}, Arg^{23} and Arg^{24}); (ii) residues belonging or not to the basic class that appear less important for the interaction with RyR1 (Lys^{19}, Lys^{20} and Thr^{26}); and (iii) a residue of the acidic face that appears to mildly affect the interaction with RyR1 (Lys^8) [23]. All of these residues are conserved in HCa; only three amino acids are different between HCa and MCa (Ala^{12}/Glu^{12}, Asp^{13}/Asn^{13} and Pro^{28}/Ile^{28}), whereas four differences are noted between HCa and IpTx A (Leu^9/Arg^9, Lys^{14}/Asn^{14}, Ser^{18}/Gly^{18} and Pro^{28}/Ala^{28}). Compared with the MCa experimental structure, the molecular model of HCa suggested that the Ala^{12}/Glu^{12}, Asp^{13}/Asn^{13} and Pro^{28}/Ile^{28} mutations have no significant effect on the backbone structure. Careful examination of the side chains of these residues showed that Asp^{13} probably interacts with five lysine residues (Lys^{14}, Lys^{19}, Lys^{20}, Lys^{22} and Lys^{30}) in HCa. The interaction between Asp^{13} and Lys^{30} may be especially privileged, thus allowing Lys^{14} to be well exposed. In IpTx A, Asp^{13} interacts with only four lysine residues (Lys^{19}, Lys^{20}, Lys^{22} and Lys^{30}), whereas in MCa, Glu^{12}, which does not possess a homologous, but rather an adjacent, residue (Glu^{13}) in HCa, also interacts with four lysine residues (Lys^{14}, Lys^{11}, Lys^{19} and Lys^{30}). Although the net global charge of MCa and IpTx A is conserved in HCa, a double mutation in the 9–14 region (Asp^{13}/Asn^{13} and Ala^{12}/Glu^{12}, Leu^9/Arg^9 and Lys^{14}/Asn^{14}) may change its electrostatic environment. This property may explain the fact that HCa exhibits a lower potency on RyR1 compared with MCa and IpTx A.

The differences in toxicity of HCa and of the two related toxins are also interesting to note. According to their respective LD_{50} values, HCa ($LD_{50} = 15\ \mu$g of toxin/1 kg of mouse) is 67 times

more toxic towards mice than MCa ($LD_{50} = 400\ \mu g$ of toxin/1 kg of mouse [6]) by i.c.v. inoculation. The neurotoxic symptoms observed in mice suggest that HCa is active in the CNS, but this requires further investigation. Among different hypotheses that may explain these differences, one suggests that HCa is more resistant to proteolysis, more efficient in terms of cell penetration to reach its pharmacological target, or possibly more potent on related RyR isoforms, such as RyR3 or RyR2, that are predominantly expressed in the CNS.

This research was supported by MRSTDC (Ministry of Scientific Research, Technology and Competency Development) and by an ACIP (Action Commune Inter Pasteurienne) project granted by the Institut Pasteur of Paris in toxin and venom researches. Single-channel analysis were supported by the National Institutes of Health grants P42 ES04699 and P42 ES05707. We are indebted to Professor François Sampieri and Dr Pascal Mansuelle (FRE 2738, CNRS-Université de la Méditerranée, IFR Jean Roche, Marseille, France) for their helpful support, to Professor Abdeladhim Ben AbdelAdhim, head of the Pasteur Institute of Tunisia, to Professor Rouholamini Najafabadi and Dr Ali Haeri, the head and reseach deputy of Pasteur Institute of Iran for their helpful advices. We also thank Dr Zakaria Ben Lasfar and his collaborators (Veterinary Laboratory, Pasteur Institute of Tunis) for providing laboratory animals. N.R. is supported by a fellowship of the Région Rhône-Alpes (France) provided by an Emergence grant.

REFERENCES

1 Radmanesh, M. (1990) Clinical study of *Hemiscorpion lepturus* in Iran. J. Trop. Med. Hyg. **93**, 327–332
2 Franzini-Amstrong, C. and Protasi, F. (1997) Ryanodine receptors of striated muscles: a complex channel capable of multiple interactions. Physiol. Rev. **77**, 699–729
3 Leong, P. and MacLennan, D. H. (1998) The cytoplasmic loops between domains II and III and domains III and IV in the skeletal muscle dihydropyridine receptor bind to a contiguous site in the skeletal muscle ryanodine receptor. J. Biol. Chem. **273**, 29958–29964
4 Zamudion, Z. F., Conde, R., Arévalo, C., Beceril, B., Martin, M. B., Valvidia, H. H. and Possani, L. D. (1997) The mechanism of inhibition of ryanodine receptor channels by imperatoxin I, a heterodimeric protein from the scorpion *Pandinus imperator*. J. Biol. Chem. **272**, 11886–11894
5 El Hayek, R., Lokuta, A. J., Avrevalo, C. and Valvidia, H. H. (1995) Peptide probe of ryanodine receptor function: imperatoxin A, a peptide from the venom of the scorpion *Pandinus imperator*, selectively activates skeletal-type ryanodine receptor isoforms. J. Biol. Chem. **270**, 28696–28704
6 Fajloun, Z., Kharrat, R., Chen, L., Lecomte, C., Di Luccio, E., Bichet, D., El Ayeb, M., Rochat, H., Allen, P. D., Pessah, I. N. et al. (2000) Chemical synthesis and characterization of maurocalcine, a scorpion toxin that activates Ca^{2+} release channel/ryanodine receptors. FEBS Lett. **469**, 179–785
7 Kuniyasu, A., Kawano, S., Hirayama, Y., Ji, Y. H., Xu, K., Ohkura, M., Furukawa, K., Ohizumi, Y., Hiraoka, M. and Nakayama, H. (1999) A new scorpion toxin (BmK-PL) stimulates Ca^{2+}-release channel activity of the skeletal-muscle ryanodine receptor by an indirect mechanism. Biochem. J. **339**, 343–350
8 Zhu, X., Zamudio, Z., Olbinski, B. A., Possani, L. D. and Valvidia, H. H. (2004) Activation of skeletal ryanodine receptors by two novel scorpion toxins from *Buthotus judaicus*. J. Biol. Chem. **279**, 26588–26596
9 Bontems, F., Roumestand, C., Gilquin, B., Menez, A. and Toma, F. (1991) Refined structure of charybdotoxin: common motifs in scorpion toxins and insect defensins. Science **254**, 1521–1523
10 Bonmatin, J. M., Bonnat, J. L., Gallet, X., Vovelle, F., Ptak, M., Reichhart, J. M., Hoffmann, J. A., Keppi, E., Legrain, M. and Achstetter, T. (1992) Two-dimensional ^1H NMR study of recombinant insect defensin A in water: resonance assignments, secondary structure and global folding. J. Biomol. NMR **2**, 235–256
11 Mosbah, A., Kharrat, R., Fajloun, Z., Renisio, J. G., Blanc, E., Sabatier, J.-M., El Ayeb, M. and Darbon, H. (2000) A new fold in the scorpion toxin family, associated with an activity on a ryanodine-sensitive calcium channel. Proteins **40**, 436–442
12 Lee, C. W., Lee, E. H., Takeuchi, K., Takahashi, H., Shimada, I., Sato, K., Shin, S. Y., Kim, D. H. and Kim, J. I. (2004) Molecular basis of the high-affinity activation of type 1 ryanodine receptors by imperatoxin A. Biochem. J. **377**, 385–394
13 Galeotti, N., Bartolini, A. and Ghelardini, C. (2003) Diphenhydramine-induced amnesia is mediated by G_i-protein activation. Neuroscience **122**, 471–478
14 Srairi-Abid, N., Mansuelle, P., Mejri, T., Karoui, H., Rochat, H., Sampieri, F. and El Ayeb, M. (2000) Purification, characterization and molecular modelling of two toxin-like proteins from the *Androctonus australis* Hector venom. Eur. J. Biochem. **267**, 5614–5620
15 Altschul, S. F., Madden, T. L., Schaffer, A. A., Zhang, J., Zhang, Z., Miller, W. and Lipman, D. J. (1997) Gapped BLAST and PSI-BLAST: a new generation of protein database search programs. Nucleic Acids Res. **25**, 3389–3402
16 Kim, D. H., Ohnishi, S. T. and Ikemoto, N. (1983) Kinetic studies of calcium release from sarcoplasmic reticulum *in vitro*. J. Biol. Chem. **258**, 9662–9668
17 Marty, I., Thevenon, D., Scotto, C., Groh, S., Sainnier, S., Robert, M., Grunwald, D. and Villaz, M. (2000) Cloning and characterization of a new isoform of skeletal muscle triadin. J. Biol. Chem. **275**, 8206–8212
18 Pessah, I. N., Stambuk, R. A. and Casida, J. (1987) Ca^{2+}-activated ryanodine binding: mechanisms of sensitivity and intensity modulation by Mg^{2+}, caffeine, and adenine nucleotides. Mol. Pharmacol. **31**, 232–238
19 Sali, A. and Blundell, T. (1993) Comparative protein modelling by satisfaction of spatial restraints. J. Mol. Biol. **234**, 779–815
20 Kleywegt, G. J. and Jones, T. A. (1996) Phi/psi-chology: Ramachandran revisited. Structure **4**, 1395–1400
21 Tosatto, S. C. (2005) The victor/FRST function for model quality estimation. J. Comput. Biol. **12**, 1316–1327
22 Zhu, S., Darbon, H., Dyason, K., Verdonck, F. and Tytgat, J. (2003) Evolutionary origin of inhibitor cystine knot peptides. FASEB J. **17**, 1765–1767
23 Estève, E., Smida-Rezgui, S., Sarkozi, S., Szegedi, C., Regaya, I., Chen, L., Altafaj, X., Rochat, H., Allen, P., Pessah, I. N. et al. (2003) Critical amino acid residues determine the binding affinity and the Ca^{2+} release efficacy of maurocalcine in skeletal muscle cells. J. Biol. Chem. **278**, 37822–37831
24 Chen, L., Estève, E., Sabatier, J.-M., Ronjat, M., De Waard, M., Allen, P. D. and Pessah, I. N. (2003) Maurocalcine and peptide A stabilize distinct subconductance states of ryanodine receptor type 1, revealing a proportional gating mechanism. J. Biol. Chem. **278**, 16095–16106
25 Altafaj, X., Cheng, E., Estève, E., Urbani, J., Grunwald, D., Sabatier, J.-M., Coronado, R., De Waard, M. and Ronjat, M. (2005) Maurocalcine and domain A of the II–III loop of the dihydroprydine receptor $Ca_v1.1$ subunit share common binding sites on the skeletal ryanodine receptor. J. Biol. Chem. **280**, 4013–4016
26 O'Reilly, F. M., Robert, M., Jona, I., Szegedi, C., Albrieux, M., Geib, S., De Waard, M., Villaz, M. and Ronjat, M. (2002) FKBP12 modulation of the binding of the skeletal ryanodine receptor onto the II–III loop of the dihydropyridine receptor. Biophys. J. **82**, 145–155
27 Stange, M., Tripathy, A. and Meissner, G. (2001) Two domains in dihydropyridine receptor activate the skeletal muscle Ca^{2+} release channel. Biophys. J. **81**, 1419–1429
28 Green, D., Pace, S., Curtis, S. M., Sakowska, M., Lamb, G. D., Dulhunty, A. F. and Casarotto, M. G. (2003) The three-dimensional structural surface of two β-sheet scorpion toxins mimics that of an α-helical dihydropyridine receptor segment. Biochem. J. **370**, 517–527
29 Gurrola, G. B., Arevalo, C., Sreekumar, R., Lokuta, A. J., Walker, J. W. and Valdivia, N. H. (1999) Activation of ryanodine receptors by imperatoxin A and a peptide segment of the II–III loop of the dihydropyridine receptor. J. Biol. Chem. **274**, 7879–7886
30 Simeoni, I., Rossi, D., Zhu, X., Garcia, J., Valdivia, H. H. and Sorrentino, V. (2001) Imperatoxin A ($IpTx_a$) from Pandinus imperator stimulates [^3H]ryanodine binding to RyR3 channels. FEBS Lett. **508**, 5–10

Received 12 September 2006/24 January 2007; accepted 12 February 2007
Published as BJ Immediate Publication 12 February 2007, doi:10.1042/BJ20061404